fractal and fractional

MDPI

Article

Supervised Neural Network Procedures for the Novel Fractional Food Supply Model

Basma Souayeh [1,2,*], Zulqurnain Sabir [3,4], Muhammad Umar [4] and Mir Waqas Alam [1,2]

1 Al Bilad Bank Scholarly Chair for Food Security in Saudi Arabia, The Deanship of Scientific Research, The Vice Presidency for Graduate Studies and Scientific Research, King Faisal University, P.O. Box 400, Al-Ahsa 31982, Saudi Arabia; wmir@kfu.edu.sa
2 Department of Physics, College of Science, King Faisal University, P.O. Box 400, Al-Ahsa 31982, Saudi Arabia
3 Department of Mathematical Sciences, United Arab Emirates University, Al Ain P.O. Box 15551, United Arab Emirates; zulqurnain_maths@hu.edu.pk
4 Department of Mathematics and Statistics, Hazara University, Mansehra 21300, Pakistan; umar_maths@hu.edu.pk
* Correspondence: bsouayeh@kfu.edu.sa

Abstract: This work presents the numerical performances of the fractional kind of food supply (FKFS) model. The fractional kinds of the derivatives have been used to acquire the accurate and realistic solutions of the FKFS model. The FKFSM system contains three types, special kind of the predator $L(x)$, top-predator $M(x)$ and prey populations $N(x)$. The numerical solutions of three different cases of the FKFS model are provided through the stochastic procedures of the scaled conjugate gradient neural networks (SCGNNs). The data selection for the FKFS model is chosen as 82%, for training and 9% for both testing and authorization. The precision of the designed SCGNNs is provided through the achieved and Adam solutions. To rationality, competence, constancy, and correctness is approved by using the stochastic SCGNNs along with the simulations of the regression actions, mean square error, correlation performances, error histograms values and state transition measures.

Keywords: fractional order; food supply model; scaled conjugate gradient; artificial neural networks; numerical solutions; Adam method

check for updates

Citation: Souayeh, B.; Sabir, Z.; Umar, M.; Alam, M.W. Supervised Neural Network Procedures for the Novel Fractional Food Supply Model. *Fractal Fract.* **2022**, *6*, 333. https://doi.org/10.3390/fractalfract6060333

Academic Editors: Libo Feng, Lin Liu and Yang Liu

Received: 22 May 2022
Accepted: 14 June 2022
Published: 16 June 2022

1. Introduction

There are various mathematical models that designate the natural phenomena based on the prey-predator investigations along with the collaborations of different species [1,2]. The functional response term in the prey-predator modelling has an important role to present that most of the prey affects the predators with the use of time. There are numerous functional responses species that have been reported in the literature, such as a ratio-dependent [3–5], Beddington–DeAngelis [6–8] and the Holling phase I to III [9,10]. One of the important models is food supply (FS), which is applied in the association of multiple prey or predators. The updated form of the FS system together with common qualitative investigations and numerous communications is presented in [11–13]. The mathematical modelling has an important role to present the dynamics of the nonlinear differential systems, e.g., SITR based coronavirus [14], dengue virus [15] and nervous stomach system [16].

In the FS chain, the role of the "Allee effects" is very important. The Allee effects defined in 1930 after the name by the famous scientist Allee. These effects allocate the progress to reduce the growing rate by using the small quantity of public. The Allee effects appear in the fishery, vertebrates, invertebrates, and plants. The Allee effects occasionally indicate the negative influences in the dispensation of population dynamics based on the fishery. The "Allee effects" have been divided into multiplication and addition [17–20]. Initially, Singh et al. described the double shape of "Allee effects" with the improved

Gower-Leslie system based on the prey predator, in which prey population shows the various junction associated with the suitable parameters. Vinoth et al. [21] formulated a mathematical model to investigate the dynamical FS system using the "Allee effect" based on the addition [22].

The aim of this work is to provide the numerical performances of the fractional kind of food supply (FKFS) model by using the stochastic procedures of the scaled conjugate gradient neural networks (SCGNNs). The stochastic solvers have been used to exploit the variety of applications in recent years. Few of them are the nonlinear dynamics of the coronavirus models [23], functional form of the singular models [24], the infectious-based HIV models [25], functional for of the delay differential system [26] and nonlinear model of the smoking [27]. The idea to implement the fraction kinds of the derivatives is to perform the accurate and realistic solutions. In fractional order models, the minute particulars based on the superfast transition and super slow evolution are examined that provides more detail of the dynamics of the system by using the fractional calculus, which is not easy to interpret by using the integer order counterparts. Additionally, the system dynamics for the index is performed by using the fractional calculus. The fractional order derivatives show much better performance as compared to the integer order with the availability of the situation. The fractional kind of the derivatives have been applied to authenticate the performance of the system using the applications of the real-world applications [28,29]. Moreover, the fractional derivatives have been extensively investigated to solve the number of applications based on the control networks, engineering, physical and mathematical systems. The implementation of the fractional calculus is performed broadly over the last 30 years by using the substantial operators, such as Weyl-Riesz [30], Caputo [31], Riemann-Liouville [32], Erdlyi-Kober [33], and Grnwald-Letnikov [34]. All these operators have their own worth and significance. However, the most widely definition of the Caputo derivative that works to solve homogeneous initial conditions as well as non-homogeneous initial conditions. The Caputo derivatives are considered easy to implement as compared to the other definitions. Bases on this fractional order applications, the authors are interested to develop the FKFS model and provide the numerical performances through the SCGNNs.

The remaining structure of the paper is given as: The FKFS system is constructed in the Section 2. The designed methodology based on the stochastic SCGNNs procedures is provided in the Section 3. The simulations of the results are provided in the Section 4. The concluding notes are given in the Section 5.

2. Mathematical FKFS System with Insights

In this section, the communication model is provided based on the two or more prey and predators. A differential FKFS system using the analysis of mutual qualitative along with the multiple relationships is given in [35,36]. Few researchers presented the multiple trophic-level of food supply systems through the structure of logistic prey $L(x)$, Holling type or Lotka–Volterra predator $M(x)$ and top-predator $N(x)$ [37–43]. The mathematical form of the three species based on the FS system is presented as [44]:

$$\begin{cases} \frac{dL(x)}{dx} = a_0 L(x) - \frac{\rho_0 L(x)M(x)}{L(x)+d_0} - \frac{k_1}{k_2+L(x)} - b_0 L^2(x), & L_0 = i_1, \\ \frac{dM(x)}{dx} = \frac{\rho_1 L(x)M(x)}{L(x)+d_1} - a_1 M(x) - \frac{\rho_2 M(x)N(x)}{M(x)+d_2}, & M_0 = i_2, \\ \frac{dN(x)}{dx} = c_3 N^2(x) - \frac{\rho_3 N^2(x)}{M(x)+d_3}, & M_0 = i_3, \end{cases} \tag{1}$$

where prey $L(x)$ and species $M(x)$ indicate the Volterra scheme that presents the population of the predator to decrease exponentially in the prey absence. The relationship of the species $N(x)$ and the prey $M(x)$ is provided by using the Leslie–Gower approach that represents the predator population reduces per capita accessibility [45,46]. a_0 and c_3 are the growth rates of $L(x)$ and $N(x)$, the environmental protection factors for $L(x)$ are d_0 and d_1, while the reduction per capita of $M(x)$ is $\frac{v_2}{2}$ described in d_2, the term a_1 shows the values of the $M(x)$, which reduces the nonappearance of $L(x)$, b_0 provides the competition strength for $L(x)$, the residual lessens for $N(x)$ based on the food shortage $M(x)$ is signified by d_3, the maximum presentations through the lessening of per capita of $L(x)$ is represented by ρ_0, ρ_1, ρ_2 and ρ_3, the hyperbolic $\frac{k_1}{k_2+L(x)}$ function shows the addictive form of the Allee effects, while k_1 and k_2 are the constant values of the Allee effects. If $k_1 < k_2$, then it means a weak Allee effect; otherwise $k_2 < k_1$, shows a strong Allee effect, the initial conditions are represented by i_1, i_2 and i_3. The mathematical form of the FKFS system is given as:

$$\begin{cases} \frac{dL^{v}(x)}{dx^{v}} = a_0 L(x) - \frac{\rho_0 L(x) M(x)}{L(x)+d_0} - \frac{k_1}{k_2+L(x)} - b_0 L^2(x), & L_0 = i_1, \\ \frac{d^{v}M(x)}{dx^{v}} = \frac{\rho_1 L(x) M(x)}{L(x)+d_1} - a_1 M(x) - \frac{\rho_2 M(x) N(x)}{M(x)+d_2}, & M_0 = i_2, \\ \frac{d^{v}N(x)}{dx^{v}} = c_3 N^2(x) - \frac{\rho_3 N^2(x)}{M(x)+d_3}, & M_0 = i_3. \end{cases} \quad (2)$$

where v shows the fractional order Caputo derivative to solve the fractional FS model given in Equation (2). The values of the fractional order derivative v are taken between 0 and 1 to present the behavior of the fractional FS model. The fractional kinds of the derivative in the FS system (2) are incoroprated to observe the minute particulars, i.e., superslow evolution and superfast transients that is not easy to interpret by using the integer order counterparts as shown in the system (1). In recent few years, the fractional calculus have been implemented in various submission, such as anomalous heat transfer [47], pine wilt disease model with convex rate [48], patterns of the spatiotemporal using the systems based on the Belousov–Zhabotinskii reaction [49], quantitative approximation of soil animal substance content using the visible/near infrared spectrometry [50], predator-prey model with herd performance [51], Hepatitis B virus mathematical model [52] and biological based population growing model using the carrying volume [53].

The novel features of the proposed SCGNNs for solving the mathematical FKFS system are defined as:

- The construction of the FKFS system is presented to examine the realistic and accurate performances of the model.
- The stochastic procedures have not been implemented before to solve the mathematical FKFS system.
- The stochastic computing SCGNNs have been applied to perform the mathematical simulations of the FKFS system using the fractional order derivatives derivative between 0 and 1.
- The accurateness of the stochastic computing SCGNNs scheme is observed through the comparison of the obtained and reference solutions.
- The performances of the absolute error (AE) in good measures indicate the accuracy and competence of the stochastic computing SCGNNs for solving the mathematical FKFS system.
- The performances based on the STs, EHs, correlation, MSE and regression approve the dependability, consistency, and reliability of the stochastic computing SCGNNs scheme for solving the FKFS system.

3. Designed SCGNNs Procedure

This section of the study provides the procedure of the stochastic computing SCGNNs scheme for the mathematical form of the FKFS system as defined in the set of system (1). The workflow diagram is provided in Figure 1 for the mathematical FKFS model using the computing SCGNNs scheme based on the three blocks, the mathematical model, designed methodology and results performances. The design performances are given in two measures.

(i) The significant procedures based on the SCGNNs are provided.
(ii) The implementation process through the designed SCGNNs for the mathematical FKFS model.

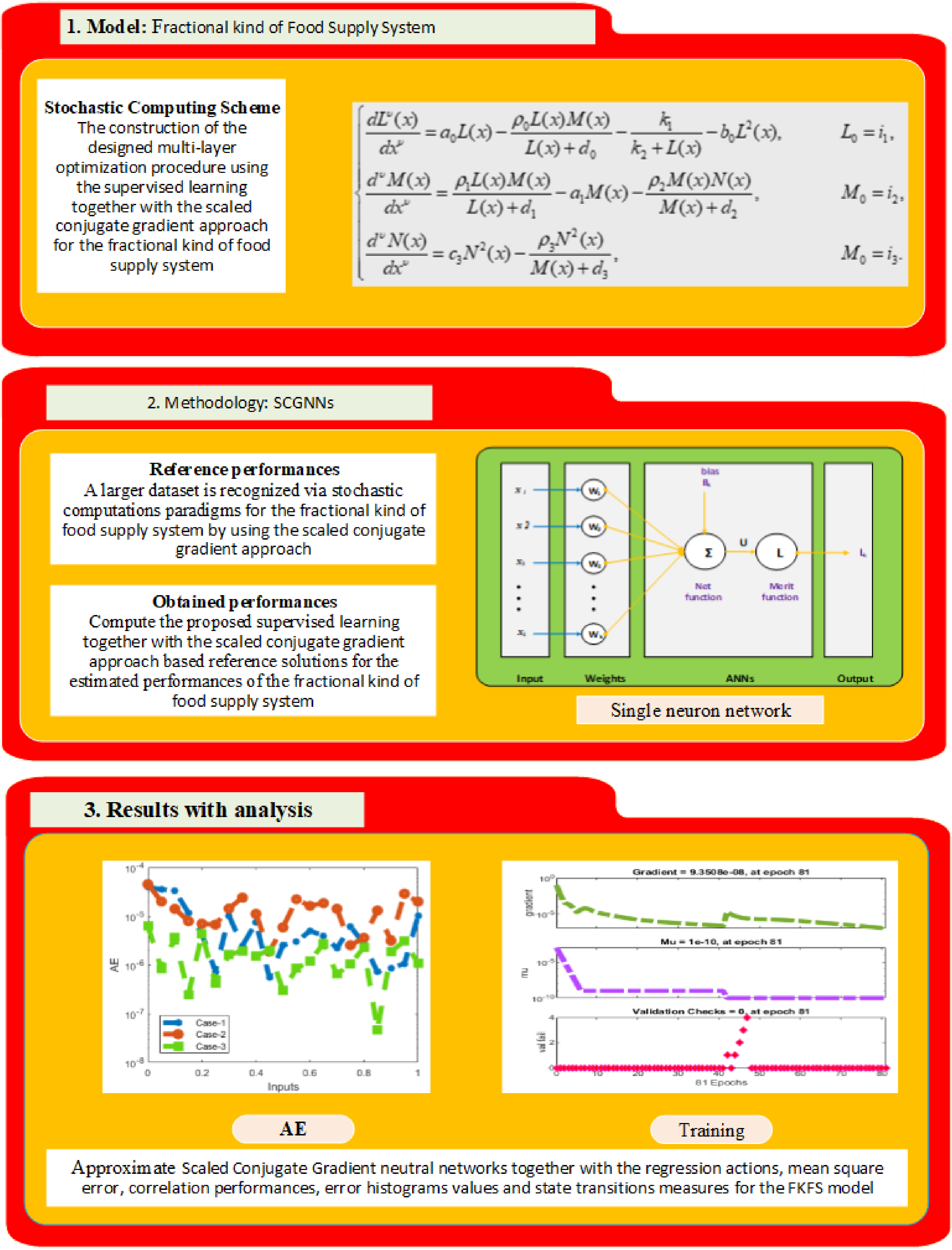

Figure 1. Workflow of the SCGNNs construction to solve the FKFS model.

The significant procedures regarding to the generalization have been provided by using the Adam scheme, while the numerical procedures are implemented with the default parameter setting to generate the model dataset. The hidden neurons have been selected 15 in this study along with the data selection for the FKFS model as 82%, for training and 9% for both testing and authorization. The artificial intelligence abilities based supervised learning SCGNNs have been performed with best cooperation in the indices, including complexity, premature convergence, overfitting and underfitting cases. Additionally, these parameters of the networks are set after exhaustive simulation studies, experience, knowledge and care and small variations in these setting results in degraded performance of the networks.

The second phase of the stochastic SCGNNs is expressed by using the generic perception based on the solo neuron model as presented in Figure 2. The Figure 2a shows the single layered neural network structure, while the designed layer construction, a single input layer vector having 15 hidden numbers of neurons in the hidden layer along with the three outcomes in the outer layer as described in Figure 2b for solving the mathematical FKFS model. The stochastic based SCGNNs are applied by using the 'Matlab' software (nftool command) for the appropriate sections of hidden neurons, testing statistics, learning methods and verification statics. Whereas the implementation performances of the SCGNNs scheme to solve the mathematical FKFS model along with the parameter setting is provided in Table 1. The networks training is performed using the proposed stochastic SCGNNs scheme, where the backpropagation is oppressed to improve the Jacobian 'JB' for the performance, i.e., MSE, to adjust the weight vectors along with the bias variables of B. The variation or modification of the decision variables with the use of scale conjugate gradient is given as:

$$\begin{aligned} JJ &= JB \times JB, \\ Je &= JB \times e, \\ dB &= \frac{-(JJ + I \times mu)}{Je}, \end{aligned}$$

where e indicates the error, and I is the identity vector. The SCGNNs scheme's parameter setting is provided in Table 1 along with the slight disparity/change/modification may result in poor performance, i.e., premature convergence. Therefore, these settings will be unified with extensive attention, after directing thorough the numerical investigation and understanding.

Table 1. Parameter setting to execute the SCGNNs procedure.

Index	**Settings**
Hidden neurons	15
Fitness goal (MSE)	0
Maximum performances of mu	10^{10}
Decreeing performances of mu	0.1
Increasing performances of mu	10
Adaptive parameter, i.e., mu	5×10^{-3}
Authentication fail amount	6
Maximum Learning Epochs	600
Minimum gradient values	10^{-6}
Training data	80%
Validation data	9%
Testing data	9%
Selection of samples	Randomly

Table 1. *Cont.*

Index	Settings
Hidden, output and layers	Single
Dataset generation solver	Adam scheme
Execution of Adam solver and stoppage criteria	Default

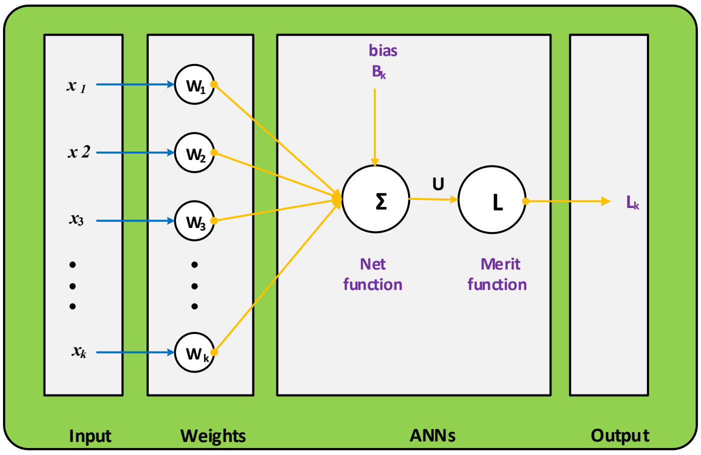

(**a**)

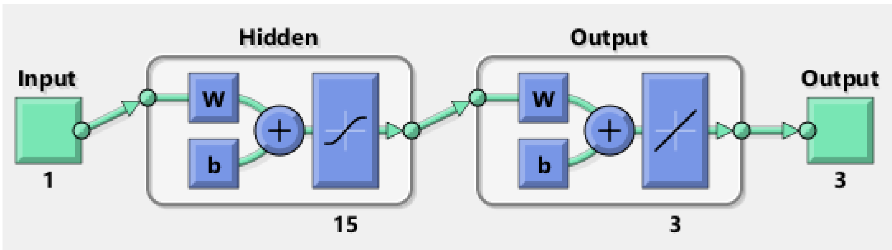

(**b**)

Figure 2. Generic and specific ANNs structure to solve the FKFS model. (**a**) Generic structure of single neuron; (**b**) Designed layer structure, a single input layer vector having 15 hidden numbers of neurons in the hidden layer along with the three outcomes in the outer layer.

4. Results of the FKFS Model

Three fractional order cases of the model have been presented by using the designed SCGNNs operator. The mathematical descriptions of these operators are given as:

Case 1: The updated form of Equation (2) based on the FKFS model by taking $\upsilon = 0.5$, $a_0 = 1.5$, $a_1 = 1$, $b_0 = 0.06$, $\rho_0 = 1$, $\rho_1 = 2$, $\rho_2 = 0.405$, $\rho_3 = 1$, $c_3 = 1.5$, $k_1 = k_2 = 0.1$, $d_0 = 10$, $d_1 = 10$, $d_2 = 10$, $d_3 = 20$ and $i_1 = i_2 = i_3 = 1.2$ is shown as:

$$\begin{cases} \frac{d^{0.5}L(x)}{dx^{0.5}} = 1.5L(x) - \frac{L(x)M(x)}{L(x)+10} - \frac{0.1}{0.1+L(x)} - 0.06L^2(x), & L_0 = 1.2, \\ \frac{d^{0.5}M(x)}{dx^{0.5}} = \frac{2L(x)M(x)}{L(x)+10} - M(x) - \frac{0.405M(x)N(x)}{M(x)+10}, & M_0 = 1.2, \\ \frac{d^{0.5}N(x)}{dx^{0.5}} = 1.5N^2(x) - \frac{N^2(x)}{M(x)+20}, & N_0 = 1.2. \end{cases} \tag{3}$$

Case 2: The updated form of Equation (2) based on the FKFS model by taking $v = 0.7$, $a_0 = 1.5$, $a_1 = 1$, $b_0 = 0.06$, $\rho_0 = 1$, $\rho_1 = 2$, $\rho_2 = 0.405$, $\rho_3 = 1$, $c_3 = 1.5$, $k_1 = k_2 = 0.1$, $d_0 = 10$, $d_1 = 10$, $d_2 = 10$, $d_3 = 20$ and $i_1 = i_2 = i_3 = 1.2$ is shown as:

$$\begin{cases} \frac{d^{0.7}L(x)}{dx^{0.7}} = 1.5L(x) - \frac{L(x)M(x)}{L(x)+10} - \frac{0.1}{0.1+L(x)} - 0.06L^2(x), & L_0 = 1.2, \\ \frac{d^{0.7}M(x)}{dx^{0.7}} = \frac{2L(x)M(x)}{L(x)+10} - M(x) - \frac{0.405M(x)N(x)}{M(x)+10}, & M_0 = 1.2, \\ \frac{d^{0.7}N(x)}{dx^{0.7}} = 1.5N^2(x) - \frac{N^2(x)}{M(x)+20}, & N_0 = 1.2. \end{cases} \quad (4)$$

Case 3: The updated form of Equation (2) based on the FKFS model by taking $v = 0.9$, $a_0 = 1.5$, $a_1 = 1$, $b_0 = 0.06$, $\rho_0 = 1$, $\rho_1 = 2$, $\rho_2 = 0.405$, $\rho_3 = 1$, $c_3 = 1.5$, $k_1 = k_2 = 0.1$, $d_0 = 10$, $d_1 = 10$, $d_2 = 10$, $d_3 = 20$ and $i_1 = i_2 = i_3 = 1.2$ is shown as:

$$\begin{cases} \frac{d^{0.9}L(x)}{dx^{0.9}} = 1.5L(x) - \frac{L(x)M(x)}{L(x)+10} - \frac{0.1}{0.1+L(x)} - 0.06L^2(x), & L_0 = 1.2, \\ \frac{d^{0.9}M(x)}{dx^{0.9}} = \frac{2L(x)M(x)}{L(x)+10} - M(x) - \frac{0.405M(x)N(x)}{M(x)+10}, & M_0 = 1.2, \\ \frac{d^{0.9}N(x)}{dx^{0.9}} = 1.5N^2(x) - \frac{N^2(x)}{M(x)+20}, & N_0 = 1.2. \end{cases} \quad (5)$$

Figures 3–7 illustrate the stochastic SCGNNs procedures for the FKFS mathematical system. Figure 3 shows the values of the STs along with the best performances of the FKFS mathematical system. The STs and MSE results based on the authentication, training and best curve measures have been demonstrated in Figure 3 using the stochastic SCGNNs procedures for the FKFS mathematical system. The obtained best measures of the FKFS model have been illustrated at iterations 81, 27 and 17 that have been performed as 7.58035×10^{-10}, 1.72965×10^{-9} and 4.49765×10^{-11}. The second half of the Figure 3 shows the gradient values using the SCGNNs scheme for the FKFS mathematical system. The performances of the gradient are found as 9.35×10^{-8}, 9.61×10^{-8} and 6.57×10^{-8}. These depictions indicate the correctness and the convergence of the SCGNNs scheme for the FKFS mathematical system. The result assessments based on the training targets, training outputs, validations targets, validation outputs, test targets, test outputs, errors and fitness curves are illustrated in the 1st half of the Figure 4. While the EHs based on the training, validation, test and zero error have been drawn in the 2nd half of the Figure 4 for the FKFS mathematical system. The EHs performances are provided as 1.68×10^{-5}, 5.79×10^{-6} and 1.05×10^{-7} for the FKFS mathematical system. Figure 5 represents the correlation performances based on the training, validation and testing in the mathematical form of the FKFS system. It is seen that the correlation measures are authenticated as 1 in the mathematical form of the FKFS system. These measures indicate the correctness of the stochastic SCGNNs procedure for the mathematical form of the FKFS model. The MSE convergence measures indicate the complexity values, training performances, validation measures, iterations, testing, and backpropagation are authenticated in Table 2 based on the mathematical form of the FKFS model.

Table 2. SCGNNs procedures for the mathematical form of the FKFS model.

Case	MSE			Epoch	Performance	Gradient	Mu	Time
	Test	Train	Validation					
1	3.56×10^{-10}	2.42×10^{-9}	7.58×10^{-10}	81	2.42×10^{-9}	9.35×10^{-8}	1×10^{-10}	02
2	2.57×10^{-9}	1.20×10^{-9}	1.72×10^{-9}	27	1.20×10^{-9}	9.61×10^{-8}	1×10^{-10}	01
3	3.28×10^{-11}	1.11×10^{-11}	4.49×10^{-11}	17	1.11×10^{-11}	6.57×10^{-8}	1×10^{-12}	01

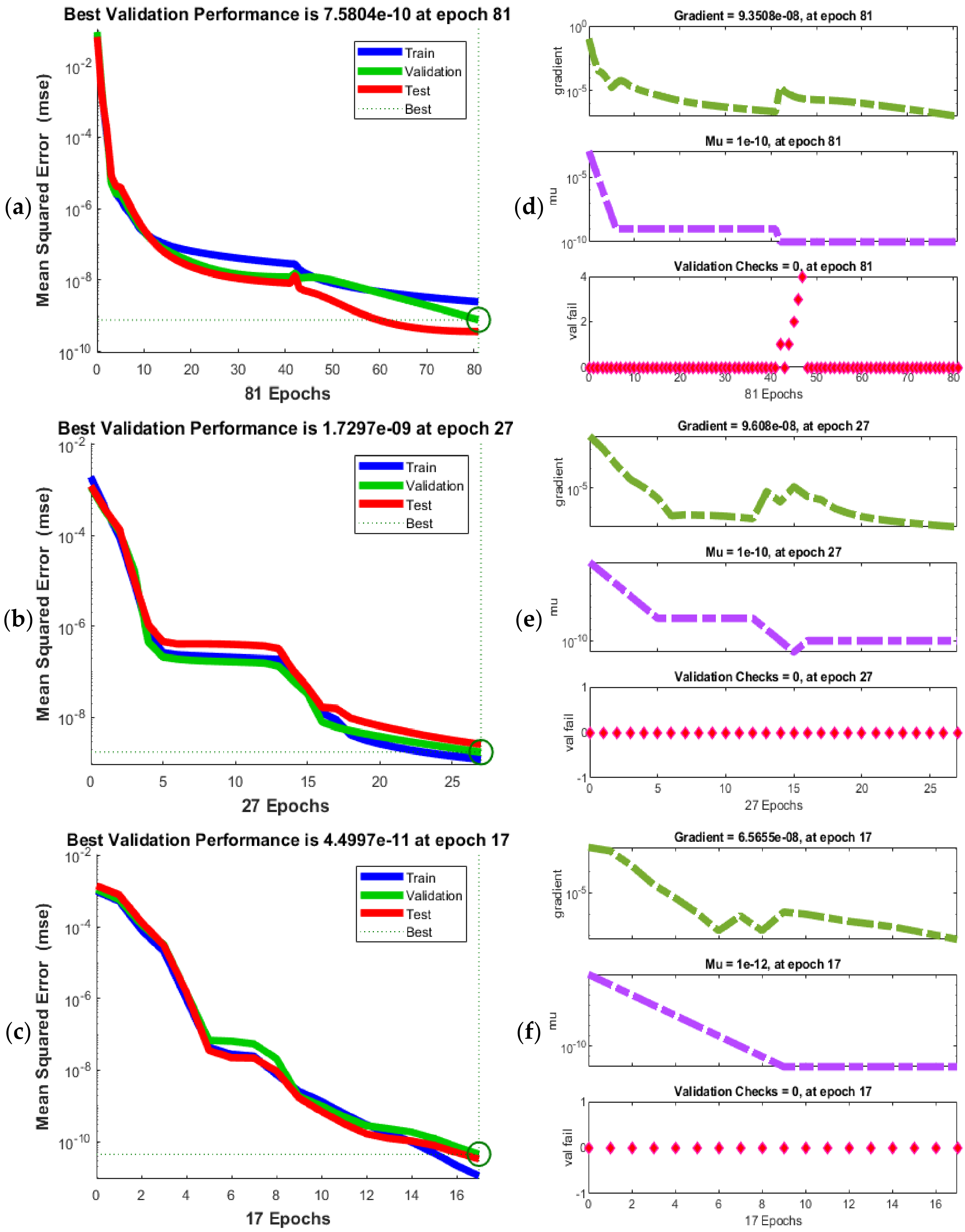

Figure 3. MSE and STs for the mathematical form of the FKFS model. (**a**) MSE for C-1; (**b**) MSE for C-2; (**c**) MSE for C-3; (**d**) EHs for C-1; (**e**) EHs for C-2; (**f**) EHs for C-3.

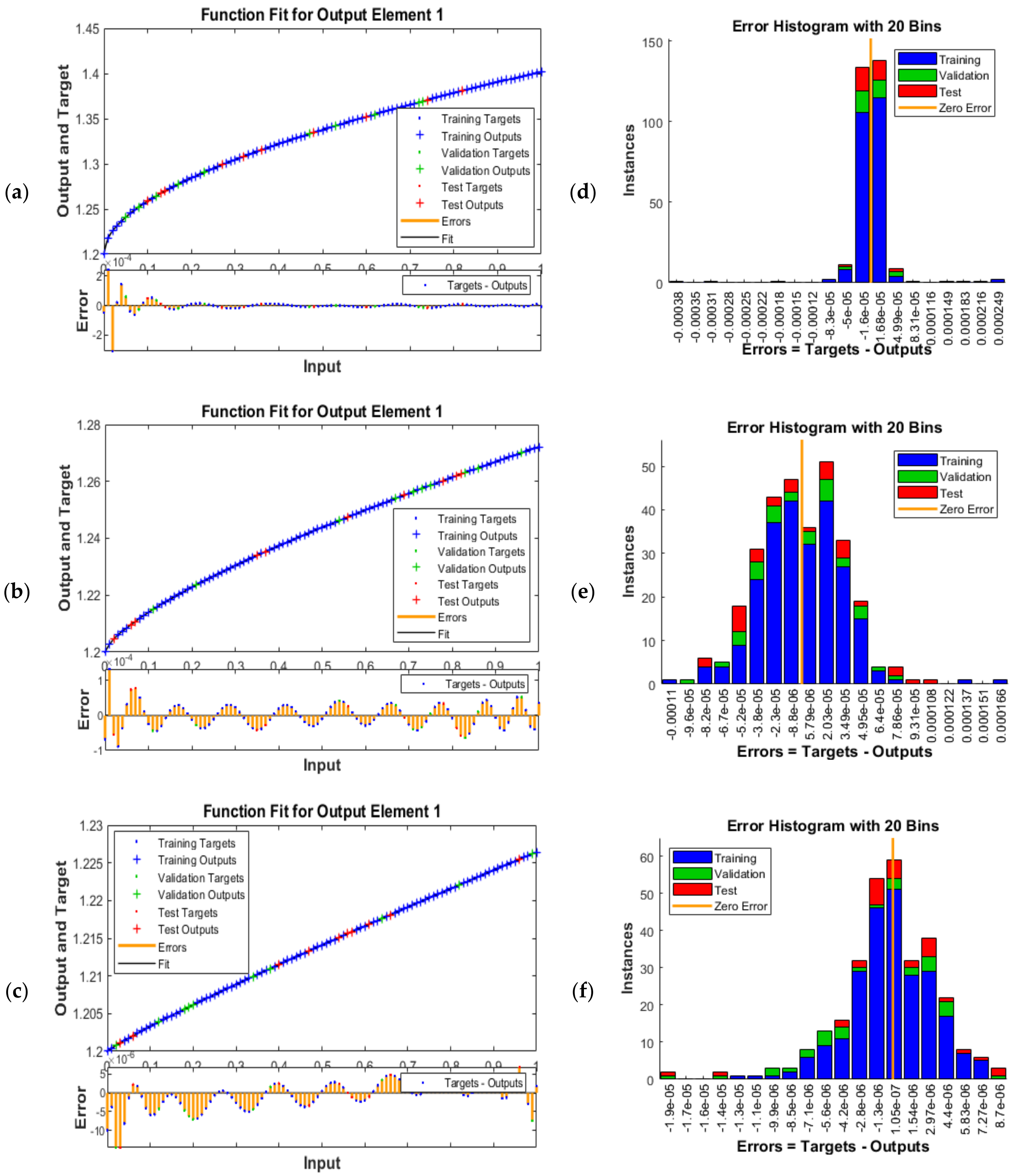

Figure 4. Results valuations and EHs for the mathematical form of the FKFS model. (**a**) Result measures for C-1; (**b**) Result measures for C-2; (**c**) Result measures for C-3; (**d**) EHs for C-1; (**e**) EHs for C-2; (**f**) EHs for C-3.

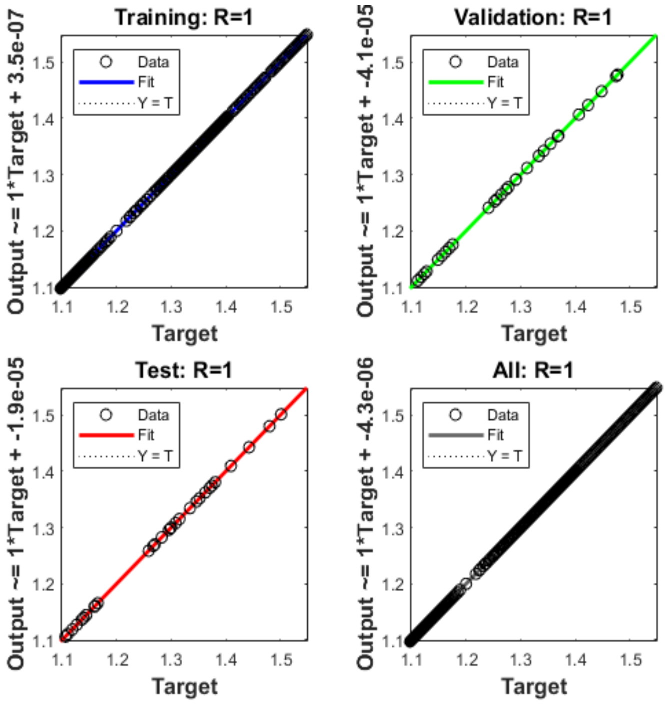

(**a**)

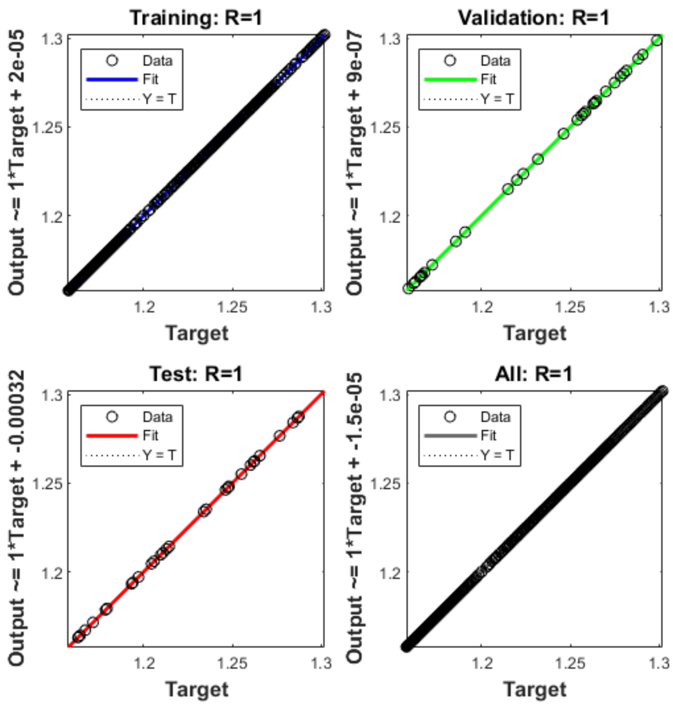

(**b**)

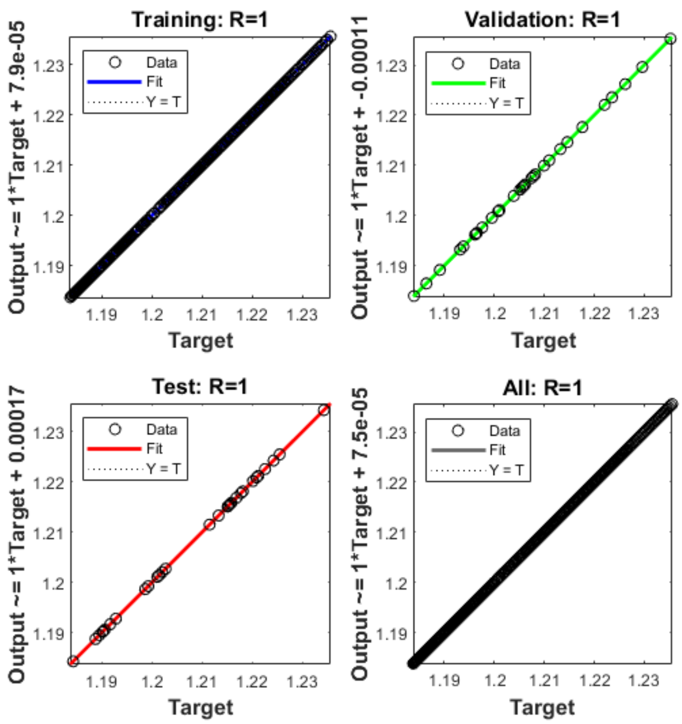

(**c**)

Figure 5. Regression performances for the mathematical form of the FKFS model. (**a**) Regression for C-1; (**b**) Regression for C-2; (**c**) Regression for C-3.

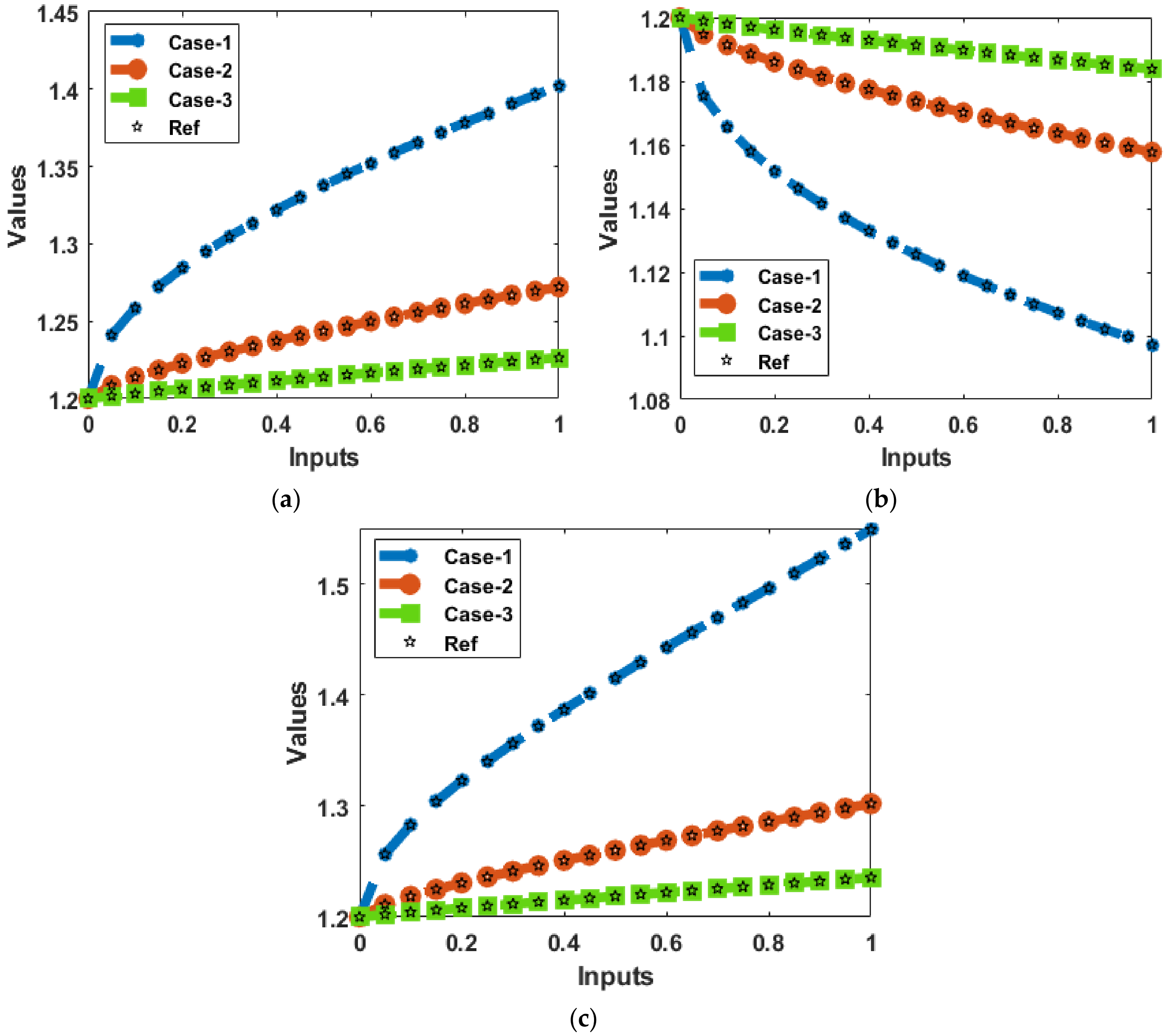

Figure 6. Results overlapping for the mathematical form of the FKFS model. (**a**) Results of the logistic prey $L(x)$; (**b**) Results of the Holling type $M(x)$; (**c**) Results for the top-predator $N(x)$.

Figures 6 and 7 indicate the comparative investigations based on the comparison of the solutions and AE performances to solve the FKFS system. Figure 6 shows the correctness of the SCGNNs scheme through the overlapping of the results for each class of the mathematical FKFS system. The AE values for each class of the mathematical FKFS system using the SCGNNs scheme are provided in Figure 7. The AE measures for the logistic prey $L(x)$ are calculated as 10^{-5} to 10^{-6}, 10^{-4} to 10^{-7} and 10^{-5} to 10^{-7} for 1st, 2nd and 3rd case of the mathematical FKFS system. The AE performances of the Holling type or Lotka–Volterra predator $M(x)$ lie as 10^{-4} to 10^{-6}, 10^{-4} to 10^{-5} and 10^{-5} to 10^{-8} for 1st, 2nd and 3rd case of the nonlinear FKFS system. The values of the AE for top-predator $N(x)$ are calculated as 10^{-4} to 10^{-6}, 10^{-5} to 10^{-6} and 10^{-5} to 10^{-8} for 1st, 2nd and 3rd case of the nonlinear FKFS system. These illustrations based on the AE authenticate the correctness of the stochastic SCGNNs LMB-NNs to solve the nonlinear FKFS system.

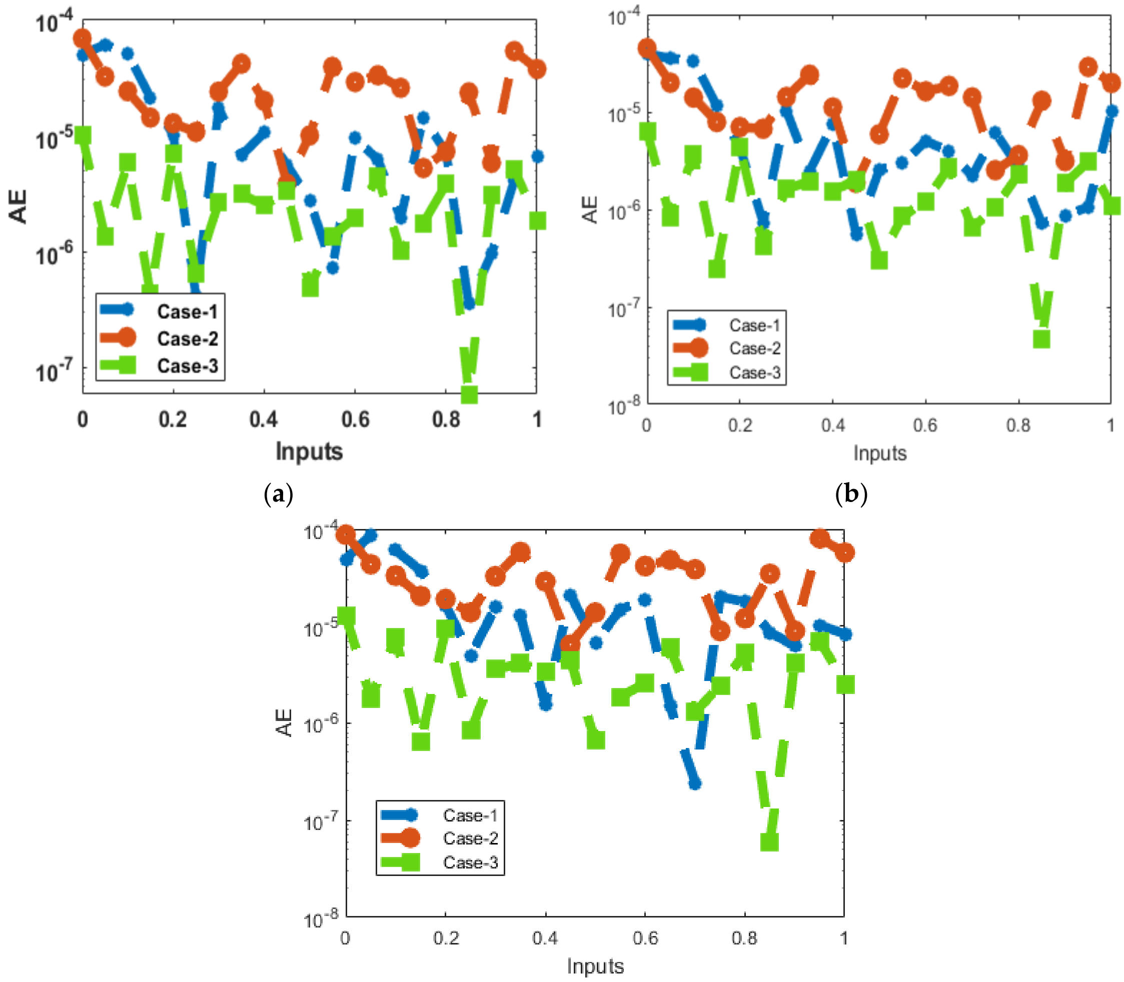

(**a**) (**b**) (**c**)

Figure 7. AE for the mathematical form of the FKFS model. (**a**) AE for the logistic prey $L(x)$; (**b**) AE for the Holling type $M(x)$; (**c**) AE for the top-predator $N(x)$.

5. Conclusions

The motive of this work is to perform the solutions of the fractional food supply model. The fractional derivatives have been used to provide the realistic and accurate solutions of the food supply mathematical model. The fractional food supply mathematical system contains three categories, special kind of the predator $L(x)$, top-predator $M(x)$ and prey populations $N(x)$. The efficient numerical performances of three different variations of the fractional food supply mathematical system have been provided by using the stochastic procedures based on the scaled conjugate gradient neural network scheme. The selection of the data for fractional food supply mathematical system is selected as 82%, for training and 9% for both testing and authorization along with the 15 numbers of neurons. The precision and accuracy of the designed SCGNNs have been provided through the achievements and reference solutions. The AE values have been calculated as 10^{-6} to 10^{-8}, which shows the exactness of the scaled conjugate gradient neural network scheme for solving the fraction food supply system. The rationality, competence, constancy, and correctness has been approved by using the stochastic SCGNNs along with the simulations of the regression actions, mean square error, correlation performances, error histograms values and state transition measures. It is also observed that by taking the fractional order values close to 1, the solutions are performed better as compared to other values. These observations have been provided in the AE graphs to solve the model.

In upcoming studies, the proposed SCGNNs scheme have been implemented to present the solutions of the lonngren-wave systems, fluid dynamical models and fractional kinds of systems.

Author Contributions: Conceptualization, B.S. and Z.S.; methodology, B.S. and M.U.; software, B.S. and Z.S.; validation, B.S. and M.U.; formal analysis, Z.S. and M.W.A.; investigation, B.S. and Z.S.; resources, B.S., Z.S., M.U. and M.W.A.; data curation, B.S. and Z.S.; writing—original draft preparation, B.S. and M.W.A.; writing—review and editing, Z.S. and B.S.; visualization, M.U. and B.S.; supervision, B.S.; project administration, B.S.; funding acquisition, B.S.; All authors have read and agreed to the published version of the manuscript.

Funding: This work was supported by Al Bilad Bank Scholarly Chair for Food Security in Saudi Arabia, the Deanship of Scientific Research, Vice Presidency for Graduate Studies and Scientific Research, King Faisal University, Saudi Arabia [Project No. CHAIR37].

Institutional Review Board Statement: Not applicable.

Informed Consent Statement: Not applicable.

Data Availability Statement: The data that support the findings of this study are available from the corresponding author upon reasonable request.

Acknowledgments: This work was supported by Al Bilad Bank Scholarly Chair for Food Security in Saudi Arabia, the Deanship of Scientific Research, Vice Presidency for Graduate Studies and Scientific Research, King Faisal University, Saudi Arabia [Project No. CHAIR37].

Conflicts of Interest: The authors declare no conflict of interest.

References

1. Damien, M.; Tougeron, K. Prey–predator phenological mismatch under climate change. *Curr. Opin. Insect Sci.* **2019**, *35*, 60–68. [CrossRef] [PubMed]
2. Berryman, A.A. The orgins and evolution of predator-prey theory. *Ecology* **1992**, *73*, 1530–1535. [CrossRef]
3. Sivasamy, R.; Sivakumar, M.; Balachandran, K.; Sathiyanathan, K. Spatial pattern of ratiodependent predator–prey model with prey harvesting and cross-diffusion, Internat. *J. Bifur. Chaos* **2019**, *29*, 1950036. [CrossRef]
4. Arditi, R.; Ginzburg, L.R. Coupling in predator–prey dynamics: Ratio-dependence. *J. Theoret. Biol.* **1989**, *139*, 311–326. [CrossRef]
5. Misra, A.K.; Dubey, B. A ratio-dependent predator–prey model with delay and harvesting. *J. Biol. Syst.* **2010**, *18*, 437–453. [CrossRef]
6. Beddington, J.R. Mutual interference between parasites or predators and its effect on searching efficiency. *J. Anim. Ecol.* **1975**, *44*, 331–340. [CrossRef]
7. DeAngelis, D.L.; Goldstein, R.A.; O'Neill, R.V. A model for tropic interaction. *Ecology* **1975**, *56*, 881–892. [CrossRef]
8. Pal, P.J.; Mandal, P.K. Bifurcation analysis of a modified Leslie–Gower predator–prey model with Beddington–DeAngelis functional response and strong Allee effect, Math. Comput. *Simulation* **2014**, *97*, 123–146.
9. Holling, C.S. The components of predation as revealed by a study of small-mammal predation of the European pine sawfly, Canad. *Entomologist* **1959**, *91*, 293–320. [CrossRef]
10. Holling, C.S. Some characteristics of simple types of predation and parasitism, Canad. *Entomologist* **1959**, *91*, 385–398. [CrossRef]
11. Hastings, A.; Powell, T. Chaos in a three-species food chain. *Ecology* **1991**, *72*, 896–903. [CrossRef]
12. Upadhyay, R.K.; Naji, R.K. Dynamics of a three species food chain model with Crowley–Martin type functional response. *Chaos Solitons Fractals* **2009**, *42*, 1337–1346. [CrossRef]
13. Jana, D.; Agrawal, R.; Upadhyay, R.K. Toppredator interference and gestation delay as determinants of the dynamics of a realistic model food chain. *Chaos Solitons Fractals* **2014**, *69*, 50–63. [CrossRef]
14. Umar, M.; Sabir, Z.; Raja, M.A.Z.; Amin, F.; Saeed, T.; Sanchez, Y.G. Integrated neuro-swarm heuristic with interior-point for nonlinear SITR model for dynamics of novel COVID-19. *Alex. Eng. J.* **2021**, *60*, 2811–2824. [CrossRef]
15. Umar, M.; Sabir, Z.; Raja, M.A.Z.; Sánchez, Y.G. A stochastic numerical computing heuristic of SIR nonlinear model based on dengue fever. *Results Phys.* **2020**, *19*, 103585. [CrossRef]
16. Sánchez, Y.G.; Sabir, Z.; Günerhan, H.; Baskonus, H.M. Analytical and approximate solutions of a novel nervous stomach mathematical model. *Discret. Dyn. Nat. Soc.* **2020**, *2020*, 5063271.
17. Brassil, C.E. Mean time to extinction of a metapopulation with an Allee effect. *Ecol. Model.* **2001**, *143*, 9–16. [CrossRef]
18. Cai, Y.; Zhao, C.; Wang, W.; Wang, J. Dynamics of a Leslie–Gower predator–prey model with additive Allee effect. *Appl. Math. Model.* **2015**, *39*, 2092–2106. [CrossRef]
19. Dennis, B. Allee effects: Population growth, critical density, and the chance of extinction. *Natur. Resour. Model.* **1989**, *3*, 481–538. [CrossRef]

20. Indrajaya, D.; Suryanto, A.; Alghofari, A.R. Dynamics of modified Leslie–Gower predator–prey model with Beddington–DeAngelis functional response and additive Allee effect. *Int. J. Ecol. Dev.* **2016**, *31*, 60–71.
21. Vinoth, S.; Sivasamy, R.; Sathiyanathan, K.; Rajchakit, G.; Hammachukiattikul, P.; Vadivel, R.; Gunasekaran, N. Dynamical analysis of a delayed food chain model with additive Allee effect. *Adv. Differ. Equ.* **2021**, *2021*, 1–20. [CrossRef]
22. Goyal, M.; Baskonus, H.M.; Prakash, A. An efficient technique for a time fractional model of lassa hemorrhagic fever spreading in pregnant women. *Eur. Phys. J. Plus* **2019**, *134*, 1–10. [CrossRef]
23. Umar, M.; Sabir, Z.; Raja, M.A.Z.; Shoaib, M.; Gupta, M.; Sánchez, Y.G. A stochastic intelligent computing with neuro-evolution heuristics for nonlinear SITR system of novel COVID-19 dynamics. *Symmetry* **2020**, *12*, 1628. [CrossRef]
24. Guirao, J.L.G.; Sabir, Z.; Saeed, T. Design and numerical solutions of a novel third-order nonlinear Emden–Fowler delay differential model. *Math. Probl. Eng.* **2020**, *2020*, 7359242. [CrossRef]
25. Umar, M.; Sabir, Z.; Raja, M.A.Z.; Aguilar, J.F.G.; Amin, F.; Shoaib, M. Neuro-swarm intelligent computing paradigm for nonlinear HIV infection model with CD4+ T-cells. *Math. Comput. Simul.* **2021**, *188*, 241–253. [CrossRef]
26. Sabir, Z.; Guirao, J.L.G.; Saeed, T. Solving a novel designed second order nonlinear Lane–Emden delay differential model using the heuristic techniques. *Appl. Soft Comput.* **2021**, *102*, 107105. [CrossRef]
27. Sabir, Z. Stochastic numerical investigations for nonlinear three-species food chain system. *Int. J. Biomath.* **2022**, *15*, 2250005. [CrossRef]
28. Yokuş, A.; Gülbahar, S. Numerical solutions with linearization techniques of the fractional Harry Dym equation. *Appl. Math. Nonlinear Sci.* **2019**, *4*, 35–42. [CrossRef]
29. İlhan, E.; Kıymaz, İ.O. A generalization of truncated M-fractional derivative and applications to fractional differential equations. *Appl. Math. Nonlinear Sci.* **2020**, *5*, 171–188. [CrossRef]
30. Ibrahim, R.W.; Momani, S. On the existence and uniqueness of solutions of a class of fractional differential equations. *J. Math. Anal. Appl.* **2007**, *334*, 1–10. [CrossRef]
31. Momani, S.; Ibrahim, R.W. On a fractional integral equation of periodic functions involving Weyl–Riesz operator in Banach algebras. *J. Math. Anal. Appl.* **2008**, *339*, 1210–1219. [CrossRef]
32. Yu, F. Integrable coupling system of fractional soliton equation hierarchy. *Phys. Lett. A* **2009**, *373*, 3730–3733. [CrossRef]
33. Diethelm, K.; Ford, N.J. Analysis of fractional differential equations. *J. Math. Anal. Appl.* **2002**, *265*, 229–248. [CrossRef]
34. Bonilla, B.; Rivero, M.; Trujillo, J.J. On systems of linear fractional differential equations with constant coefficients. *Appl. Math. Comput.* **2007**, *187*, 68–78. [CrossRef]
35. Feng, G.; Yin, D.; Jiacheng, L. Neimark–Sacker Bifurcation and Controlling Chaos in a Three-Species Food Chain Model through the OGY Method. *Discret. Dyn. Nat. Soc.* **2021**, *2021*, 6316235. [CrossRef]
36. Mondal, A.; Pal, A.K.; Samanta, G.P. Stability and bifurcation analysis of a delayed three species food chain model with Crowley-Martin response function. *Appl. Appl. Math. Int. J.* **2018**, *13*, 8.
37. Thakur, N.K.; Ojha, A.; Jana, D.; Upadhyay, R.K. Modeling the plankton–fish dynamics with top predator interference and multiple gestation delays. *Nonlinear Dyn.* **2020**, *100*, 4003–4029. [CrossRef]
38. El-Owaidy, H.M.; Ragab, A.A.; Ismail, M. Mathematical analysis of a food-web model. *Appl. Math. Comput.* **2001**, *121*, 155–167. [CrossRef]
39. Freedmanand, H.I.; So, J.H. Global stability and persistence of simple food chains. *Math. Biosci.* **1985**, *76*, 69–86. [CrossRef]
40. Kuznetsov, Y.A.; Rinaldi, S. Remarks on food chain dynamics. *Math. Biosci.* **1996**, *134*, 1–33. [CrossRef]
41. Freedman, H.I.; Waltman, P. Mathematical analysis of some three-species food-chain models. *Math. Biosci.* **1977**, *33*, 257–276. [CrossRef]
42. Muratori, S.; Rinaldi, S. Low-and high-frequency oscillations in three-dimensional food chain systems. *SIAM J. Appl. Math.* **1992**, *52*, 1688–1706. [CrossRef]
43. Rinaldi, S.; Bo, S.D.; de Nittis, E. On the role of body size in a tri-trophic metapopulation model. *J. Math. Biol.* **1996**, *35*, 158–176. [CrossRef]
44. Aziz-Alaoui, M.A. Study of a Leslie–Gower-type tritrophic population model. *Chaos Solitons Fractals* **2002**, *14*, 1275–1293. [CrossRef]
45. Leslie, P.H.; Gower, J.C. The properties of a stochastic model for the predator-prey type of interaction between two species. *Biometrika* **1960**, *47*, 219–234. [CrossRef]
46. Upadhyay, R.K.; Iyengar, S.R.K.; Rai, V. Chaos: An ecological reality? *Int. J. Bifurc. Chaos* **1998**, *8*, 1325–1333. [CrossRef]
47. Yang, X.J.; Ragulskis, M.; Tana, T. A new general fractional-order derivataive with Rabotnov fractional-exponential kernel applied to model the anomalous heat transfer. *Therm. Sci.* **2019**, *23*, 1677–1681. [CrossRef]
48. Shah, K.; Alqudah, M.A.; Jarad, F.; Abdeljawad, T. Semi-analytical study of Pine Wilt Disease model with convex rate under Caputo–Febrizio fractional order derivative. *Chaos Solitons Fractals* **2020**, *135*, 109754. [CrossRef]
49. Owolabi, K.M.; Hammouch, Z. Spatiotemporal patterns in the Belousov–Zhabotinskii reaction systems with Atangana–Baleanu fractional order derivative. *Phys. A Stat. Mech. Its Appl.* **2019**, *523*, 1072–1090. [CrossRef]
50. Hong, Y.; Liu, Y.; Chen, Y.; Liu, Y.; Yu, L.; Liu, Y.; Cheng, H. Application of fractional-order derivative in the quantitative estimation of soil organic matter content through visible and near-infrared spectroscopy. *Geoderma* **2019**, *337*, 758–769. [CrossRef]
51. Ghanbari, B.; Djilali, S. Mathematical and numerical analysis of a three-species predator-prey model with herd behavior and time fractional-order derivative. *Math. Methods Appl. Sci.* **2020**, *43*, 1736–1752. [CrossRef]

52. Din, A.; Li, Y.; Khan, F.M.; Khan, Z.U.; Liu, P. On Analysis of fractional order mathematical model of Hepatitis B using Atangana–Baleanu Caputo (ABC) derivative. *Fractals* **2022**, *30*, 2240017. [CrossRef]
53. Srivastava, H.M.; Dubey, V.P.; Kumar, R.; Singh, J.; Kumar, J.; Baleanu, D. An efficient computational approach for a fractional-order biological population model with carrying capacity. *Chaos Solitons Fractals* **2020**, *138*, 109880. [CrossRef]